CHAPTER 1

INTRODUCTION

The need for trace analyses in complex matrices is becoming more apparent. There are, however, many difficulties surrounding this type of analysis. For example, solutions with trace impurities in a matrix solution that has a high salt content or a high concentration of total dissolved solids present a problem when analysing by spectroscopic techniques. In contrast, the high salt content is generally beneficial in improving the conductivity of the solution when using an electrochemical technique. This technique also provides the sensitivity needed and can be selective depending on the background electrolyte used. This project was aimed at finding whether an electrochemical technique would be suitable to solve this problem. In addition, electrochemical techniques offer the ability to do speciation, which spectroscopic techniques are not always suitable to do.

The peak potentials of a number of metals are close together, but it is often relatively easy to carry out the determination of several metals in one run, if they are present in similar concentrations. It is, however, more complicated to determine a trace amount in the presence of a large excess of an interfering substance. There are many different kinds of interferences that need to be recognised in these situations. Surface-active agents could adsorb onto the electrode surface which could poison the electrode. Substances could react with the electrode material. Two substances could be deposited together at a given potential and influence each other during the stripping process, for example, their peaks could overlap. The analyte could be deposited while another substance that is present in excess, which stays in solution, undergoes a simultaneous electrode reaction. During the stripping process, the substance in the solution undergoes the reverse electrode reaction that may interfere owing to the appearance of a wave or a broad peak in the vicinity of the analyte peak [1].

The selectivity of an electrochemical analysis can be improved in a number of ways. A preliminary separation could take place, such as a solvent extraction, coprecipitation, volatilisation, chromatographic techniques, electrophoresis and so on. However, this is not preferable as it requires a significantly longer analysing time, more contamination could occur and it is often not suited to trace determination. Electrochemistry has a "built-in" preconcentration step, namely pre-electrolysis, which is more suitable. The pre-electrolysis conditions, the stripping technique and the choice of the electrode material could all improve selectivity. It also enhances the sensitivity greatly.

Stripping analysis consists of two main steps, namely the preconcentration step and the stripping step. In the preconcentration step, the analyte is accumulated onto or into the electrode. In the stripping step, the accumulated material is oxidised or reduced back into solution. The response recorded in the latter step is proportional to the amount of accumulated analyte which, in turn, is proportional to the bulk concentration. There are various stripping techniques such as anodic stripping voltammetry (ASV), cathodic stripping voltammetry (CSV), potentiometric stripping analysis (PSA), adsorptive stripping voltammetry (AdSV) and so on [2]. Only ASV and AdSV will be looked at in detail here as they were the techniques used in this project.

ASV entails the reduction of a metal ion to the metal during the preconcentration step. This is achieved by applying a potential, that is more cathodic than the standard potential of the least easily reduced metal to be analysed, for a specified time period. A metallic layer forms on the surface of the electrode or an amalgam is formed when a mercury electrode is used. This step generally involves forced convection to improve the mass transport of the analyte to the surface of the electrode. The convection is stopped and a rest period of a couple of seconds is implemented to ensure that the stripping step occurs in a quiescent solution and to establish a uniform concentration within the mercury if a mercury electrode is used. A positive-going potential scan is then applied and the accumulated species are then reoxidised. The metals are stripped from the electrode in an order that is a function of their standard potential. This gives

rise to anodic peak currents which are measured. The concentration of the metal can then be deduced from the heights (or areas) of the peaks produced [2].

The concept for AdSV is very much the same as that for ASV. In the case of a metal determination, a metal chelate is formed and this is adsorbed onto the surface of the electrode at a particular potential for a specified time period. Stripping is achieved by a negative-going potential scan and reduction occurs, either through the metal or the ligand. The current response is proportional to the surface concentration of the analyte, which is proportional to the bulk concentration in solution. Many other surface-active substances can be analysed in this way [2].

Complexing agents provide various ways of improving selectivity of the stripping methods. A suitable complexing agent could shift the deposition potential of an interfering metal so that it will not deposit at the electrode, or move the stripping peaks further apart. The analyte could also be complexed, resulting in an adsorption of this complex at the electrode. It is necessary to know the electrode reactions of the complexing agents themselves under the conditions of the determination, to avoid possible interferences.

Pre-electrolysis together with matrix exchange is a powerful way to improve the selectivity. After pre-electrolysis from the sample solution, the stripping process is carried out in another electrolyte that is free of interfering species. The best way to perform a matrix exchange is by using a flow system. In this manner the deposit is not exposed to air when the solution is changed and the deposit does not undergo mechanical forces and possible losses when the electrode is removed from the one solution and inserted into another. An electrochemical detector can readily be inserted into the conduits of a flow system and thus on-line analysis is also made possible. Other advantages of a flow system include convective mass transport, automation, increased precision, reduced analysis time and reduced contamination.

In these trace analyses, it is not only the selectivity that is an issue, but also the sensitivity. Generally some form of enrichment of the analyte is required. Electrolytic accumulation is a simple and convenient way to both isolate and preconcentrate the component of interest. This can be done in a number of ways, for example the deposition of the analyte on the surface or into the electrode, the adsorption of a complex onto the surface of the electrode, the use of modified electrodes and so on.

Two different matrices were looked at in the project, namely a zinc electrolyte and high purity gold. The impurities analysed for were cobalt and arsenic respectively.

1.1) DETERMINATION OF COBALT IN ZINC ELECTROLYTES

There are several grades of zinc on the market, the purest of which is produced by the electrolytic process [3]. The main procedures in producing zinc involve mining and concentrating the ore. This is then roasted to form zinc oxide which is dissolved in dilute sulphuric acid. The solution is purified to remove unwanted impurities and electrolysis is carried out on this solution. It is at this point where impurities present even in very small quantities could have extremely undesirable effects. Once depleted, the zinc sulphate solution and the generated sulphuric acid are returned to the leaching step. This cyclic circuit is susceptible to the accumulation of impurities [3,4].

Elements that could have a deleterious effect on zinc electrowinning and that are generally present in significant quantities are iron, cobalt, nickel, copper, arsenic, antimony, germanium, tin, selenium, tellurium, cadmium, silver, lead, chlorine, fluorine and manganese [3,5-8]. The type and quantity of impurities present would depend on the location of the ore body. Some of the problems experienced due to the presence of these impurities are: reduced current efficiencies, a poor deposit morphology, the co-deposition with zinc, the redissolution of deposited zinc, the lowering of the hydrogen over-voltage or the zinc deposit could adhere to the cathode [3,5,9,10]. Elements such as sodium, potassium, calcium and magnesium may be present in large quantities

without having detrimental effects [3]. It is therefore important to be able to analyse the electrolyte before the electrolysis step to prevent any of the above mentioned problems.

Cobalt as an impurity was particularly looked at in this study. The presence of cobalt causes the formation of round holes in the zinc deposit as a result of redissolution of zinc [3,9]. This redissolution is caused by an increased amount of hydrogen evolution due to cobalt present. [11] It has also been reported that it decreases the current efficiency [12]. Cobalt can be tolerated to about 10 $mg.l^{-1}$ in the absence of other impurities, but its harmful effects are increased by the presence of other elements such as germanium [3]. It is therefore estimated that a maximum of 0.3 $mg.l^{-1}$ cobalt is acceptable [12]. In theory cobalt should be removed by the addition of zinc dust, but in practice it does not remove sufficient amounts. A number of other additives could be used for cobalt removal, such as potassium antimony tartrate, antimony trioxide, Nitroso-Beta-Naphthol, hot copper-arsenic-zinc dust or an aqueous solution of sodium ethyl xanthate [3].

In this project, cobalt was determined as its DMG (dimethylglyoxime) complex at a hanging mercury drop electrode (HMDE) and hence AdSV was used. This would curb problems experienced with cobalt at a mercury electrode such as the irreversibility of the redox process and the poor sensitivity of stripping methods due to the low solubility of cobalt in mercury [12-14]. This would also give some selectivity as the reduction potentials of cobalt and zinc are similar.

The work by Mrzljak *et al.* [12] was used as a basis for this part of the project as they also analysed for cobalt in a zinc electrolyte. This was to ensure that the flow system designed for this project was working well and this was best done using a method that had been proven to work previously. The project could then be extended to unknown scenarios. Their work takes many things into account. The cobalt sensitivity was enhanced by forming the DMG complex. The interference from the extremely high zinc concentrations present were reduced in two ways, namely, by complexing the zinc with

sodium citrate which moves the zinc reduction peak to more negative potentials and by utilising a matrix exchange method where stripping occurs in a comparatively uncontaminated solution. [12]

Mrzljak *et al.* [12] used a bottom-drain cell displayed in figure 1.1. The zinc electrolyte was first diluted six times with a supporting electrolyte. The sample was then injected directly over the HMDE from the flow adapter and during this time the analyte was collected at the working electrode that was held at a fixed potential. Due to the greater density of the sample versus the stripping electrolyte contained in the cell, the sample sank to the bottom of the cell and stripping occurred in a relatively uncontaminated solution, thus reducing zinc interference. The contaminated stripping electrolyte was then drained and replaced by fresh electrolyte [12]. This cell design restricted its use to samples with fairly high specific gravities, whereas the cell designed for this project was aimed at producing a cell that would be more versatile (refer to chapter 3).

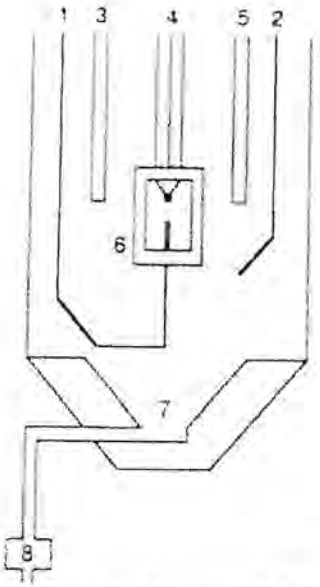

Figure 1.1: Schematic diagram of the bottom-drain cell used by Mrzljak *et al* [12]. (1) Sample inlet line; (2) nitrogen purge line; (3) reference electrode; (4) Metrohm HMDE; (5) auxiliary electrode; (6) PAR 310 flow adapter; (7) sample-electrolyte drain to waste; (8) control valve

Included in the flow system was a deoxygenation system. This was to remove dissolved oxygen present in solution which interferes in the application of electroanalytical techniques. A semi-permeable membrane set-up was used due to its efficiency in oxygen removal and its ability to be used in flow systems (refer to chapter 4).

1.2) THE DETERMINATION OF ARSENIC IN HIGH PURITY GOLD

It is necessary to be able to determine the amount of impurities in gold in order to assess the value, to check its physical properties for other uses, for example in medicine and in microelectronics, and to establish its point of origin. The typical content of trace impurities in high purity gold is represented in table 1.1 [15].

Table 1.1: Typical content of trace impurities in high purity gold [15]

Element	**Concentration / $\mu g.g^{-1}$**	**Element**	**Concentration / $\mu g.g^{-1}$**
Cu	0.5	Zn	0.5
Fe	0.6	As	0.24
Pb	1.2	Sb	0.12
Ni	0.6	Sn	0.05
Co	0.015	Bi	0.06
Mn	0.019	Al	6.0
Cd	0.1	Se	<0.01
Cr	0.5	Te	<0.01
Pd	1.0	V	<0.01
Rh	0.5	Pt	<0.01

The minerals arsenopyrite ($FeS_2.FeAs_2$), realgar (As_2S_2) and orpiment (As_2S_3) are associated with some gold ores [21]. Since arsenic is slightly soluble in gold forming an alloy, it is often found as an impurity in gold.

Work has been done by several authors [15-20] in this regard by different techniques and mechanisms. E. Ivanova *et al.* [15-18] used flame AAS and ETAAS to determine the impurities in high purity gold. They used different sample preparations to remove the matrix element, such as sorption onto a strong-base anion exchanger [16]; the use of chelating sorbents of the pyrazolone type [17]; solvent extraction with methylethylketone/chloroform [15]; and the reduction of gold to its elemental state by hydrazine hydrate [18]. Karadjova *et al.* [19] also looked at the reduction of gold to its elemental state by various organic compounds, namely, hydrazine hydrate, hydroquinone, ascorbic acid and oxalic acid. They found that oxalic acid performed the best as there was little coprecipitation of the trace elements to be determined. ICP-AES has been used to determine the impurities in gold [19]. The spontaneous reduction of gold in the nebuliser system caused clogging of the system and led to strong memory effects. ICP-MS was also employed [19,20] and it was found that there were several spectral, matrix and molecular ion interferences. These include producing the interfering polyatomic $^{49}Ar^{35}Cl^{-}$ on monoisotropic $^{75}As^{+}$, gold suppressing the analyte signal by its space-charge effect and the total dissolved solids had to be less than 0.5% (m/m) to prevent deposition of material on the skimmer cones to avoid drift and loss of sensitivity [23]. However, detection limits were still reported at 1 $\mu g.g^{-1}$ for most impurities except for arsenic and antimony, for which the limit of detection was 5 $\mu g.g^{-1}$.

Arsenic has been determined in many other matrices by various methods and techniques. Spectrophotometric (colourometric) methods are widely used for arsenic determination due to the simplicity and low cost. However they have limited use because of the poor sensitivity. Techniques that have been employed for the sensitive determination of arsenic include: hydride generation atomic absorption spectrometry (HG-AAS) [22-26], flame atomic absorption spectrometry (FAAS) [27], hydride generation inductively coupled plasma atomic emission spectrometry (HG-ICP-AES) [28], high performance liquid chromatography hydride generation atomic fluorescence spectrometry (HPLC-HG-AFS) [29], capillary electrophoresis (CE) [30], potentiometric stripping analysis (PSA) [31,32] and voltammetry [33-36]. Ways to separate the arsenic

from interferences or to preconcentrate the arsenic were also studied [22,37,38], but these methods were tedious, time consuming and could lead to contamination.

Voltammetry was used to detect arsenic (III) in a gold sample in this project. A gold film electrode was used which was formed by depositing a gold film onto a glassy carbon electrode. A preparation procedure for this electrode was developed in order to produce a uniform, non-porous film (refer to chapter 2).

The gold in the sample was complexed with cyanide to form the extremely stable aurous cyanide complex ($Au(CN)_2^-$) which has a stability constant of $2x10^{38}$ [21]. Due to the slow kinetics of reduction for this complex, the deposition potential for the gold is shifted in a negative direction. This was done to prevent the gold from plating together with the arsenic onto the electrode. The ratio of the gold and arsenic concentrations in the sample is of the order of $4x10^6$. Due to this large difference, the method would be very insensitive if the gold and arsenic were plated simultaneously, as it would be predominantly gold accumulated on the electrode surface. The formation of the gold (I) cyanide complex would involve dissolving the gold sample in an alkaline cyanide solution in the presence of oxygen.

Matrix exchange was performed to prevent the passivation of the gold film electrode and also to improve the sensitivity of the detection. A wall-jet cell (WJC) was employed for this purpose (refer to chapter 3). In a WJC, the flow of a jet of fluid strikes the plane electrode perpendicularly and flows radially over its surface [39-44]. The same deoxygenation system as described previously was used, but solutions needed to be sparged with nitrogen beforehand to achieve the necessary extent of deoxygenation.

1.3) REFERENCES

1) A.J. Bard and L.R. Faulkner, Electrochemical Methods - Fundamentals and Applications, John Wiley and Sons, 1980

2) P.T Kissinger and W.R. Heineman, Laboratory Techniques in Electroanalytical Chemistry, 2nd Edition, Marcel Dekker Inc., New York, 1996
3) G.T. Wever, JOM, 11 (1959) 130
4) J.A. Gonzalez-Dominguez and R.W. Lew, JOM, 47 (1995) 34
5) M. Karavasteva, Hydromet., 35 (1994) 391
6) M. Geissler and R. Da Maia, Fresnius Z. Anal. Chem., 330 (1988) 624
7) E.S. Pilkington, C. Weeks and A.M. Bond, Anal. Chem., 48 (1976) 1665
8) A.M. Bond, R.W. Knight and O.M.G. Newman, Anal. Chem., 60 (1988) 2445
9) L. Muresan, G. Maurin, L. Oniciu and D. Gaga, Hydromet., 43 (1996) 345
10) A.M. Bond, B.V. Pfund and O.M.G. Newman, Anal. Chim. Acta, 277 (1993) 145
11) C. Cachet, C. Le Pape-Rerolle and R. Wiart, J. Appl. Electrochem., 29 (1999) 813
12) R.I. Mrzljak, A.M. Bond, T.J. Cardwell, R.W. Cattrall, R.W. Knight, O.M.G. Newman, B.R. Champion, J. Hey and A. Bobrowski, Anal. Chim. Acta, 281 (1993) 281
13) B. Pihlar, P. Valenta and H.W. Nurnberg, Fresenius Z. Anal. Chem., 307 (1981) 337
14) S.B. Adeloju, A.M. Bond and M.H. Briggs, Anal. Chim. Acta, 164 (1984) 181
15) E. Ivanova, N. Jordanov, I. Havesoz, M. Stoimenova and S. Kadieva, Fresenius J. Anal. Chem., 336 (1990) 501
16) E. Ivanova and H. Berndt, Fresenius J. Anal. Chem., 340 (1991) 419
17) E. Ivanova, O. Todorova and M. Stoimenova, Fresenius J. Anal. Chem., 344 (1992) 316
18) E. Ivanova, I. Havesoz, H. Berndt and G. Schaldach, Fresenius J. Anal. Chem., 336 (1990) 320
19) A. Karadjova, S. Arpadjan and L. Jordanova, Fresenius J. Anal. Chem., 367 (2000) 146
20) S.M. Graham and R.V.D. Robert, Talanta, 41 (1994)1369
21) Gold metallurgy in South Africa, Chamber of Mines of SA, Johannesburg, 1972
22) T. Kubota, T. Yamaguchi and T. Okutani, Talanta, 46 (1998) 1311
23) P. Becotte-Haigh, J.F. Tyson, E. Denoyer and M.W. Hinds, Spectrochim. Acta Part B, 51 (1996) 1823

24) R.I. Ellis, N.G. Sundin, J.F. Tyson, S.A. McIntosh, C.P. Hanna and G. Carnrick, Analyst, 123 (1998) 1697
25) J. Stummeyer, B. Harazim and T. Wippermann, Fresenius J. Anal. Chem., 354 (1996) 344
26) S. Karthikeyan, T. Prasada Rao and C.P.S. Iyer, Talanta, 49 (1999) 523
27) A.R.K. Dapaah and A. Ayame, Anal. Chim. Acta, 360 (1998) 43
28) B. Jamoussi, M. Zafzouf and B. Ben Hassine, Fresenius J. Anal. Chem., 356 (1996) 331
29) Z. Slejkovec, J.T. van Elteren and A.R. Byrne, Talanta, 49 (1999) 619
30) E. P. Gil, P. Ostapczuk and H. Emons, Anal. Chim. Acta, 389 (1999) 9
31) J.H. Aldstadt and A.F. Martin, Analyst, 121 (1996) 1387
32) S.B. Adeloju, T.M. Young, D. Jagner and G.E. Batley, Anal. Chim. Acta, 381 (1999) 207
33) H. Li and R.B. Smart, Anal. Chim. Acta, 325 (1996) 25
34) G. Henze, W. Wagner and S. Sander, Fresenius J. Anal. Chem., 358 (1997) 741
35) D. Sancho, M. Vega, L. Deban, R. Pardo and G. Gonzalez, Analyst, 123 (1998) 743
36) P.H. Davis, G.R. Dulude, R.M. Griifin, W.R. Matson and E.W. Zink, Anal. Chem., 50 (1978) 137
37) I. Eguiarte, R. M. Alonso and R.M. Jimenez, Analyst, 121 (1996) 1835
38) W. Wisniewski, Hydromet., 46 (1997) 235
39) A.J. Bard, Electroanalytical Chemistry, Volume 16, Marcel Dekker Inc., 1989
40) W.J. Albery and C.M.A. Brett, J. Electroanal. Chem., 148 (1983) 211
41) W.J. Albery and C.M.A. Brett, J. Electroanal. Chem., 148 (1983) 201
42) J. Wang and B.A. Freiha, Anal. Chem., 57 (1985) 1776
43) R.G. Compton, A.C. Fisher, M.H. Latham, R.G. Wellington, C.M.A. Brett and A.M.C.F. Oliveira Brett, J. Appl. Electrochem., 23 (1993) 98
44) P. Laevers, A. Hubin, H. Terryn and J. Vereecken, J. Appl. Electrochem., 25 (1995) 1017

CHAPTER 2

ELECTRODES

A three-electrode system was used in the various set-ups, in other words they had a working electrode, an auxiliary electrode and a reference electrode. This leads to compensated and uncompensated resistance. The uncompensated iR drop is basically the resistance of the working electrode itself and the solution resistance between the working electrode and the reference electrode [1,2].

2.1) WORKING ELECTRODES

The main properties required by a working electrode, in order to give high accuracy, reproducibly, sensitivity and low detection limits, are:

- electrochemical inertness over a broad potential interval, [3]
- high oxygen and hydrogen overpotential, [3]
- stability for infinite time periods, [1,4]
- good signal-to-noise ratios, i.e. the residual current must be low but the current response to electroactive species must be high, [4]
- low ohmic resistance [3] and
- the possibility of easy and sufficient surface regeneration. [3]

Needless to say, such an electrode does not exist, thus choosing a suitable working electrode is a compromise to best fit the experiment.

2.1.1) Mercury Electrodes for the Determination of Cobalt

2.1.1.1) Theory

It has been shown that cobalt(II) is potentiostatically adsorbed onto a mercury electrode as its DMG complex [5]. The advantage of using a mercury electrode is that it has a high hydrogen overpotential [4,6]. The down side is the toxicity of mercury and the limited potential range for anodic reactions due to mercury oxidation from approximately 0.4 V [7]. There is also strong interference from oxygen [8,9] and

the electrode can easily be fouled when exposed to complex samples [10]. This proved to be the most feasible electrode for these studies and its accessible potential range was as required, but some deoxygenation would be necessary.

When comparing the HMDE and the thin film mercury electrode (TFME) the main difference is that the HMDE has a fresh, smooth surface for each analysis, thus leading to very reproducible results, and there is no need for polishing or reactivation. The HMDE also has a linear response over a wide range of concentrations, without exhibiting saturation or interference effects [11]. The double layer charging current is, however, high due to the large surface area of a mercury drop [4]. A TFME is more sensitive [12] and gives better resolution than a HMDE as peak widths are narrower [13]. However, the experimental complexity and time is increased and there are problems maintaining a constant active surface area [9]. It is also more difficult to obtain a reproducible and stable electrode surface [14]. The HMDE produces broad stripping peaks as the metal slowly diffuses from the interior to the surface of the drop. This can be overcome by using high frequency techniques, such as ac or pulse techniques, which give narrower stripping peaks because it is only the metal on the surface of the drop that is looked at [12]. In the case of AdSV, adsorption on the analyte only takes place on the surface of the electrode. In flow cells the TFME is easier to manage as the HMDE produces vibration or turbulence at high flow rates, which leads to poor performance [4,9,10,15].

Considering the pros and cons of the HMDE and the TFME, it was decided to utilise the HMDE due to its ease of use and readily renewable surface, especially when analysing the complex zinc electrolyte, hence avoiding many surface related problems. Using differential pulse stripping voltammetry could enhance the sensitivity. The major problems that had to be overcome was to design a stable flow system using a HMDE and provide on-line deoxygenation.

2.1.1.2) Experimental

An EG&G Princeton Applied Research Model 303 Static Mercury Drop Electrode (SMDE) (EG&G, New Jersey, USA) was used as shown in figure 2.1. The BAS 100B/W Electrochemical Workstation (Bioanalytical Systems, West Lafayette, USA) remotely controlled it.

Figure 2.1: EG&G Princeton Applied Research Model 303 Static Mercury Drop Electrode

The area of the mercury drop could be calculated from the mass of the drops, assuming a spherical shape. This was done by Peterson [7] for the PARC SMDE and the results he found are shown in table 2.1. The drop mass was an average of 20 determinations and the areas calculated represent typical areas for these electrodes.

Table 2.1: The electrode areas calculated for various drop sizes for the PARC SMDE [7]

Drop size	**Drop mass / mg**	**Drop area / cm^2 x 10^2**
Small	1.2	0.96
Medium	2.5	1.56
Large	5.4	2.61

A schematic diagram of the mechanical assembly of the SMDE is shown below in figure 2.2 [16]. The mercury flows from the reservoir through a vertical hole into the top of the solenoid body and down around the valve stem. The compression spring continuously exerts a downward force on the retaining ring so that the polyurethane tip at the end of the valve stem seals the top end of the capillary. When the solenoid is activated, the valve stem is lifted and mercury can then flow down the capillary. The drop forms quickly to the required size, which is controlled by the duration the valve is lifted, and then remains that size until it is dislodged. The metallic parts that are in contact with the mercury are made of stainless steel to prevent contamination and the non-metallic materials do not react with mercury [16].

The SMDE needed some maintenance before it could be used as it was standing for a number of years. The old mercury was drained and the whole system was cleaned because much of the mercury had oxidised. The reservoir was filled with clean triply distilled mercury. (In all cases the mercury was collected and disposed of in the appropriate manner.) The polyurethane seal on the tip of the valve stem was also remade as it had become hard over the years and was indented by the capillary. This was moulded from an epoxy resin (Pratley) glue because it could adhere to the tip of the valve stem and also had a similar pliability to the polyurethane tip, hence it would make a good seal with the top of the capillary. A new capillary was carefully installed so that there was no air trapped in it. The capillaries had a bore of approximately 0.15 mm. A new glass sleeve with a Vycor frit for the Ag/AgCl reference electrode was filled with fresh saturated silver chloride solution, ensuring that there were no trapped air bubbles, and was also put in place. This reference electrode has a potential no more than 50mV more positive than the standard calomel electrode [16] and was only used in the cup-cell arrangement.

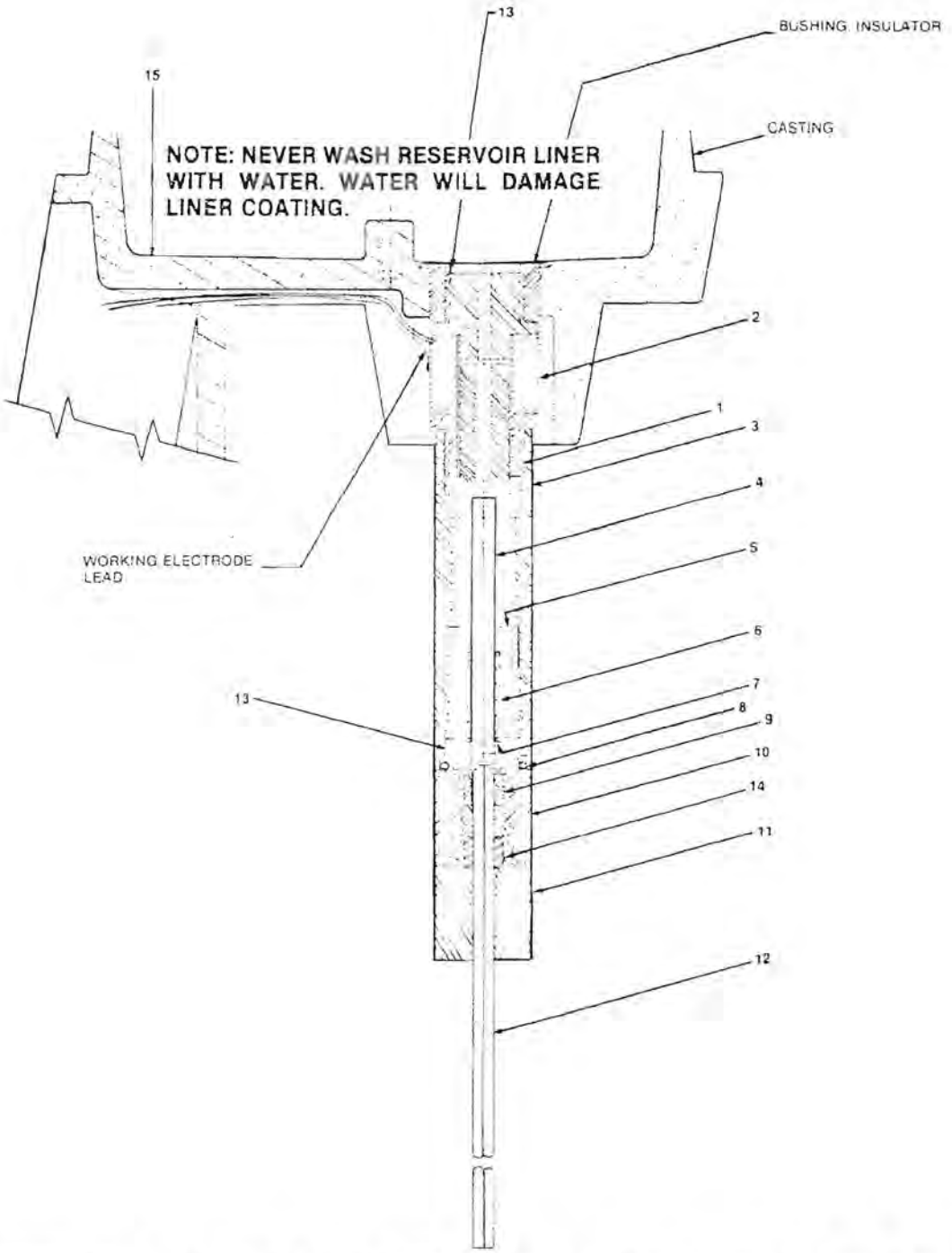

Figure 2.2: Schematic diagram of the mechanical assembly of the SMDE. The labels are as follows: (2) solenoid body, (3) valve body, (4) valve stem assembly, (5) valve guide bushing, (6) compression spring, (7) retaining ring, (8) O-ring, (9) capillary seal, (10) valve seat, (11) capillary nut, (12) capillary assembly, (14) ferrule support and (15) reservoir liner.

On occasion, the capillaries were replaced when the drops would not adhere to the tip of the capillary. This was probably due to solution creeping up the mercury capillary resulting in a narrower neck which was unable to hold the weight of the drop [6]. The capillary was cleaned by aspirating 10% (v/v) hydrofluoric acid through it for about 15 seconds, followed by copious amounts of deionised water. A siliconising solution contained 5% (v/v) dichlorodimethylsilane in carbon tetrachloride. It was aspirated halfway up the bore of the capillary and allowed to stand for an hour. The solution was removed by aspiration and the capillaries were then dried in an oven at 65°C overnight [16].

The SMDE was used in the HMDE mode. At the start of each run the drop knocker is activated, the old mercury drop is dislodged off the end of the capillary and a new drop is formed. A small or medium drop size was generally used. A large mercury drop led to mechanical instability in the flow cell and it is also reported that the greater the working electrode's surface area, the greater the extent of noise [1].

2.1.2) Thin Gold Film Electrodes for the Determination of Arsenic

2.1.2.1) Theory

Several electrode materials have been used for the determination of arsenic by stripping techniques. These include the HMDE with the aid of Cu(II) or Se(IV) to preconcentrate the As(III) by way of forming intermetallic compounds on the electrode and the codeposition with copper on a platinum electrode [19]. But the most suitable electrode material has been found to be gold, whether it be a solid gold disk or a thin film gold electrode [19-28]. The use of a mercury electrode on its own was unsuccessful as arsenic is sparingly soluble in mercury [25] and the arsenic oxidation peak appeared as a shoulder on the mercury oxidation wave which was of little analytical use [19,22]. Silver was also found to be unsuitable due to the arsenic peak emerging as a shoulder [22]. Arsenic had been determined at a platinum electrode, but gold was found to be superior [20,22]. Gold has a higher hydrogen overpotential than platinum, so interference from hydrogen was reduced. Gold electrodes also display better reversibility of the electrode reactions which results in higher and sharper oxidation peaks for arsenic [19,22].

The problem with using solid electrodes, such as gold, is that the electrode response is strongly dependent on the past history, pretreatment and oxide film formation [19,22]. A huge problem is the lack of understanding of the true electrode surface conditions and their effect on the electrode process [29], as well as the difficulty to reproduce the electrode surface [30]. It is important that the electrode surface is clean and that deleterious effects such as adsorption, electropolymerisation, fouling and poisoning be avoided [29,31]. The accumulation of foreign material on the electrode results in reduced electrode activity. Methods have been devised to rejuvenate the working electrode activity, for example, chemical treatments, potential excursions and mechanical polishing [29,32,33]. Mechanical polishing has been shown to temporarily alter the electrode response such that an equilibration period is necessary to stabilise it [29]. Electrochemical pretreatment of the electrode is very convenient and it produces electrode stability and a decrease in the extent of overpotential [33].

In many respects the thin gold film and the thin mercury film behave in much the same manner. These are usually plated on a glassy carbon electrode (GCE) substrate. This is due to glassy carbon having low background currents over a wide potential range, a high hydrogen overpotential, low porosity, extreme hardness and high chemical inertness [31]. Glassy carbon is a gas-impermeable carbon material made from phenolic resins by heating it in an inert atmosphere. Different conditions give slightly different properties of the glassy carbon, therefore it is difficult to compare results for different electrodes. The microstructures of different electrodes vary significantly, even when they are cut from the same rod. They exhibit randomly scattered surface defects in the form of very small craters, ruts and pits which cannot be removed by polishing. It has been shown that the smooth areas consist of pure carbon whereas metals (for example Fe, Mg, Al, Si, V, Ni, and Cr) can be found in the micropores [31]. Other substrates that have been used are impregnated graphite [34], pyrolytic graphite[19], platinum [32] and solid gold [34]. It is important that the effects observed are not due to reactions with the substrate material; thus the film should not be porous or have imperfections [32].
The GCE surface had to be treated as any solid electrode to ensure reproducibility and a low background current [34,35]. The performance of a gold film on a GCE was

markedly affected by the condition of the GCE surface prior to gold deposition and by the amount of gold that was deposited [30]. Mercury plates onto the active sites on the GCE, leaving the less active sites uncovered. It appears that gold deposits in a similar manner. As the extent of oxidation on the GCE expanded, the number of active sites were reduced and the gold tended to deposit in larger particles at fewer sites, so that the specific surface available for analyte deposition is decreased [30]. Contrary to expectation, surfaces with greater roughness and irregularities gave more reproducible results for mercury films [31]. This is probably due to a larger number of active sites on the electrode surface and it would be expected that the gold film behave in a similar way. This also yielded a more mechanically stable film. It was shown that merely wiping the used gold film from the GCE surface with a tissue before replating a new film was insufficient as the sensitivity between analyses dropped more rapidly [30]. More rigorous methods such as potential cycling or polishing were necessary [19,26,27,30-36].

A thin film shows gradual deterioration due to mechanical stresses, the deposition and/or adsorption of contaminants and so on [37]. Usually a single gold film could be used for a number of determinations [25,26,30], but at times deterioration between analyses is too great [19]. It was found that if electrolytes contained high concentrations of chloride, the gold film would degrade quickly. This was because of the $AuCl_4^-$ complex formation, which resulted in the gold film being dissolved. A make-up procedure was run between analyses where a small amount of gold was plated again. The presence of impurities also had a profound effect on the behaviour of the gold film electrode [19].

In a flow cell, the film thickness should be less than the diffusion layer thickness. This is easily satisfied in a wall-jet cell where the diffusion layer thickness is of the order of 10 μm for flow rates between 1-4 $ml.min^{-1}$ [35]. The thickness of the film can be calculated if it can be approximated that the atoms are uniformly deposited. This is done by measuring the limiting current (i_{lim}) when the film is stripped from the substrate and applying the following equation [35]:

$$\ell = \frac{i_{lim} M}{nF\pi R^2 \rho}$$

where M is the atomic mass of gold (in the case of a gold film), n is the number of electrons, F is Faraday's constant, R is the radius of the electrode and ρ is the density of gold. A film has been deposited at a wall-jet electrode [38], but it has also been shown that a mercury film was partly removed by the impinging solution [31]. It is thus important that the film is mechanically stable in a hydrodynamic cell.

2.1.2.2) Experimental

A number of different substrate preparation and gold plating regimes were adopted by various authors [19,25-27,30,33,34,36]. This work encompassed plating a gold film onto a glassy carbon substrate to produce a uniform, lustrous film.

The plating solution used for the formation of the gold film electrode was a 50 $mg.l^{-1}$ gold (III) solution in 5% (v/v) sulphuric acid. This was obtained by dissolving 99.99% gold in aqua regia to produce a 10 $g.l^{-1}$ gold solution. It was then diluted and the appropriate amount of sulphuric acid was added.

The film was not plated in the flow cell mainly owing to three reasons which are discussed below. It was previously shown that plating in a stationary solution produced a lustrous gold surface, whereas if plating took place in a hydrodynamic solution the film was more like a brown powder [19,25]. The whole electrode surface is not equally accessible in a wall-jet cell which could affect the evenness of the film. Due to the cost of the plating solution, it could be reused if plated from a vial. However, the electrode is not exposed to air when plated in the flow cell. Gold is not affected by oxygen at any temperature, whether moisture is present or not [21]. Thus the exposure of the gold film electrode to air for very short periods should not have detrimental effects. In the case of mercury films, it was reported that the removal of the electrode after plating occurred produced a patchy texture because the mercury droplets coalesced [31]. This was not observed with the gold film that was plated.

Plating took place in the BAS C2 Cell Stand (Bioanalytical Systems, West Lafayette, USA). The vial was filled with 8 ml of gold plating solution. The working electrode was a 3 mm diameter GCE, the reference electrode was a RE-5 silver/silver chloride electrode and the counter electrode was a platinum wire, all supplied by BAS. The solution was sparged with nitrogen for 5 minutes before plating commenced and a

nitrogen blanket was maintained above the surface of the solution during plating. It was discovered that lifting and reinserting the GCE in and out of the solution about three times after sparging removed any bubbles that were lodged on the electrode surface. If the nitrogen bubbles were not removed, the gold film that was plated had holes in it where the bubbles were situated.

Initially the GCE was polished with 1 μm alumina. This was done as specified in the BAS electrode polishing and care pamphlet [17]. A microcloth was stuck to a glass block and the cloth was wetted with some water. Some alumina paste was added to the surface of the cloth and the electrode was polished by placing it perpendicular to the glass block and moving it in the shape of a figure-8. This was done without applying excessive pressure. After a short period the electrode was rotated 120° and the figure-8 motion was continued for the same length of time. This was repeated once more to ensure an evenly polished surface. The electrode was then rinsed in water and ultrasonicated for 2 minutes in water to remove any residual alumina or abraded glassy carbon particles. It was then rinsed successively in water, 1 mol.l^{-1} nitric acid and finally water again.

Deposition of the gold film took place as suggested by Sun *et al.* [19] at –200 mV for 4 minutes in a quiescent solution. The reproducibility of the film was tested by analysing an arsenic (III) solution in 20% (v/v) hydrochloric acid. It was also suggested [19] that a "make-up" plating run be done between analyses to restore the gold film. This was done in the deoxygenated plating solution at +500 mV for 10 s, once again ensuring that there were no bubbles on the electrode surface.

The first tests performed in a vial (not the flow cell) showed erratic results as depicted in figure 2.3. A 5 mg.l^{-1} arsenic (III) solution was tested at various deposition times in a stirred or quiescent solution. The solution was first sparged with nitrogen for 5 minutes. The deposition potential was –300 mV and the final potential was 100 mV. DPSV was done with a scan rate of 50 mV.s^{-1}, a pulse height of 50 mV, a pulse width of 50 ms, a pulse period of 200 ms and a sample width of 20 ms. Stirring took place at a setting of 5 on the C2 Cell Stand and a 15 s quiet time was employed. It can be seen that the longer arsenic accumulation times showed a greater general increasing trend in the peak current. This was probably due to the arsenic not being totally

stripped off the electrode during the stripping step and hence there was some accumulation at the electrode. For the shorter deposition times, results were more reproducible when no stirring occurred during the accumulation step. This could be due to two phenomena, namely the increased noise during stirring and thus during the plating step, and the increase in mass transport led to a greater amount of arsenic being deposited and once again the stripping step may not have removed it all.

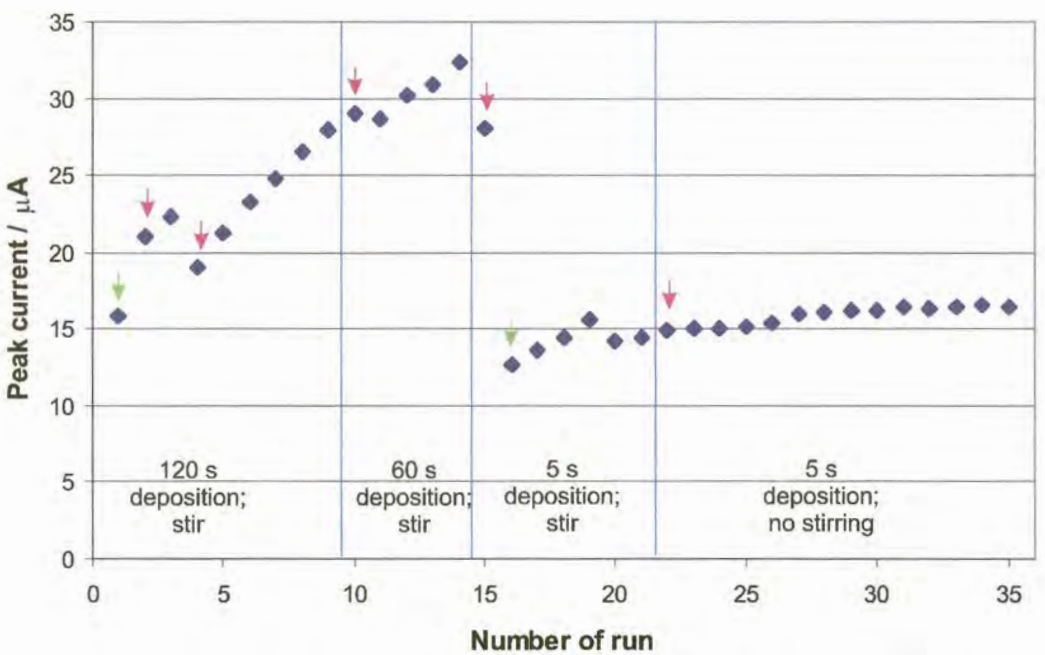

Figure 2.3: Testing the reproducibility of the gold film electrode. The green arrows represent plating the gold film before the analysis and the pink arrows represent doing a make-up plating run before the analysis.

The gold film electrode was stored in a deoxygenated solution of 0.1 mol.l^{-1} sulphuric acid overnight. Once again the peak currents were measured, as before, in arsenic (III) solutions. It was found that after sparging the arsenic solutions, lifting and reimmersing the working electrode in and out of the solution gave more reproducible results. The results in figure 2.4 show the peak currents for different concentrations of arsenic (III) solutions applying a deposition time of 5 s to quiescent solutions. The RSD is less than 5% for all concentrations which is acceptable. The correlation coefficient for the calibration was 0.9938, as shown in figure 2.5. This graph implied that when no arsenic was present, the peak height should be –6.9 μA. This would be

impossible, hence the integrity of the results were questioned. Positive results were that the peak currents for the 2 mg.l^{-1} arsenic solution were reproducible, whether a make-up plating run was done before the determination or not. It also showed that storing the gold film electrode in the deoxygenated sulphuric acid solution seemed to stabilise the electrode. When the gold film was looked at, it was more of a brown powdery coating with a relatively high resistance.

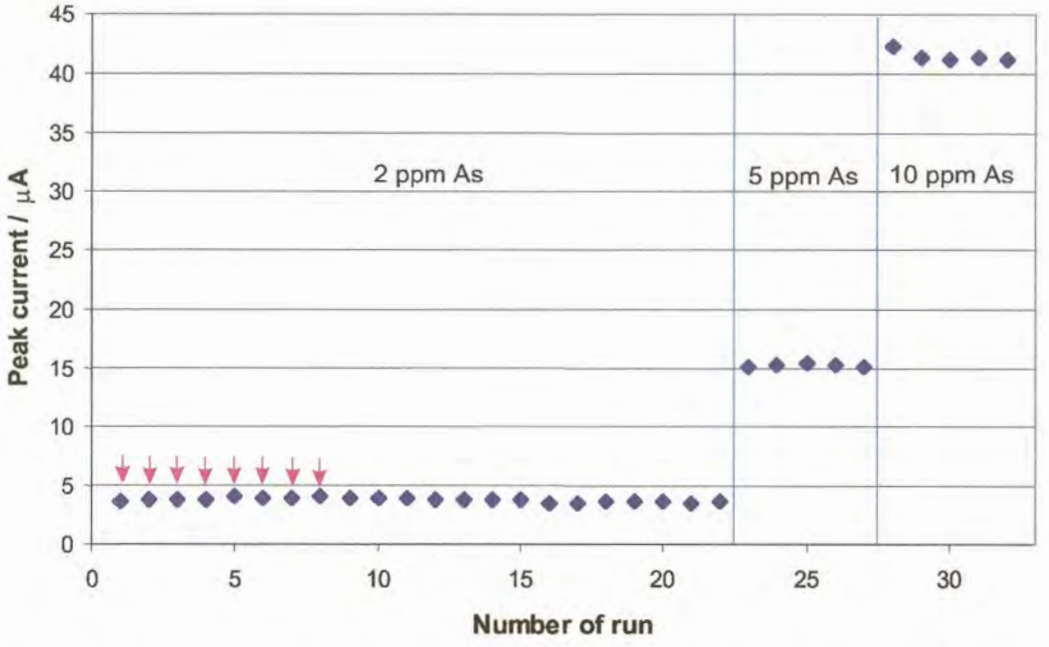

Figure 2.4: Testing the reproducibility of the gold film electrode at various arsenic (III) concentrations. The pink arrows represent a make-up plating run before the analysis.

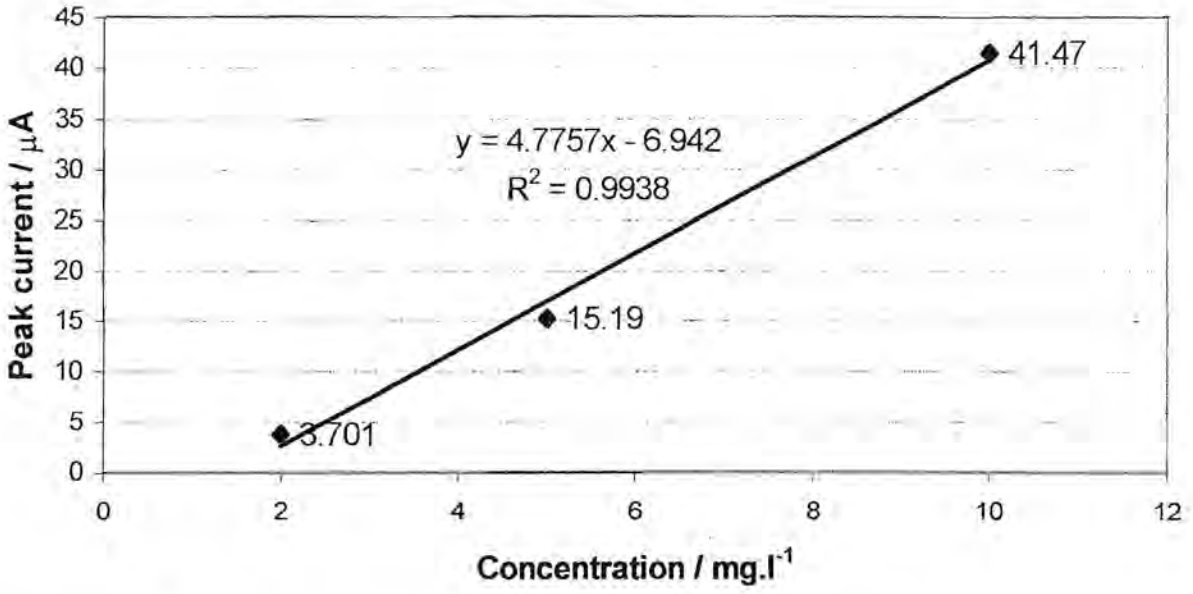

Figure 2.5: The graph of peak current versus arsenic (III) concentration

It was decided to reconsider the plating potential for the gold film. A cyclic voltammogram was obtained at the GCE in the gold plating solution. This is displayed in figure 2.6. The potential at which the gold was being plated (-200 mV) was in the diffusion-controlled region. It was decided to try and plate the gold film in the activation-controlled potential region. Thus plating occurred at potentials from 730 to 790 mV in quiescent solutions. This did not produce the film properties required. Plating in stirred solutions was also attempted as this kept conditions further away from diffusion-control, but with no success.

When the gold film was studied under a microscope at about 40 times magnification, the film was very irregular and there were white crystalline deposits on the surface, as illustrated in figure 2.7. The uneven film could be due to the electrode not being totally perpendicular during plating, or that the whole electrode surface was not uniformly activated. The white crystalline material was thought to be residual alumina from the polishing step. After the electrode was polished with 1 µm alumina, rinsed and ultrasonicated twice, the material was still there. It appeared as though it was embedded in the GCE. The electrode was then successively polished with 9 µm, 3 µm and 1 µm diamond paste with rinsing and ultrasonicating between the

different size abrasives. Lastly the electrode was polished with 1 μm alumina. The white material was removed.

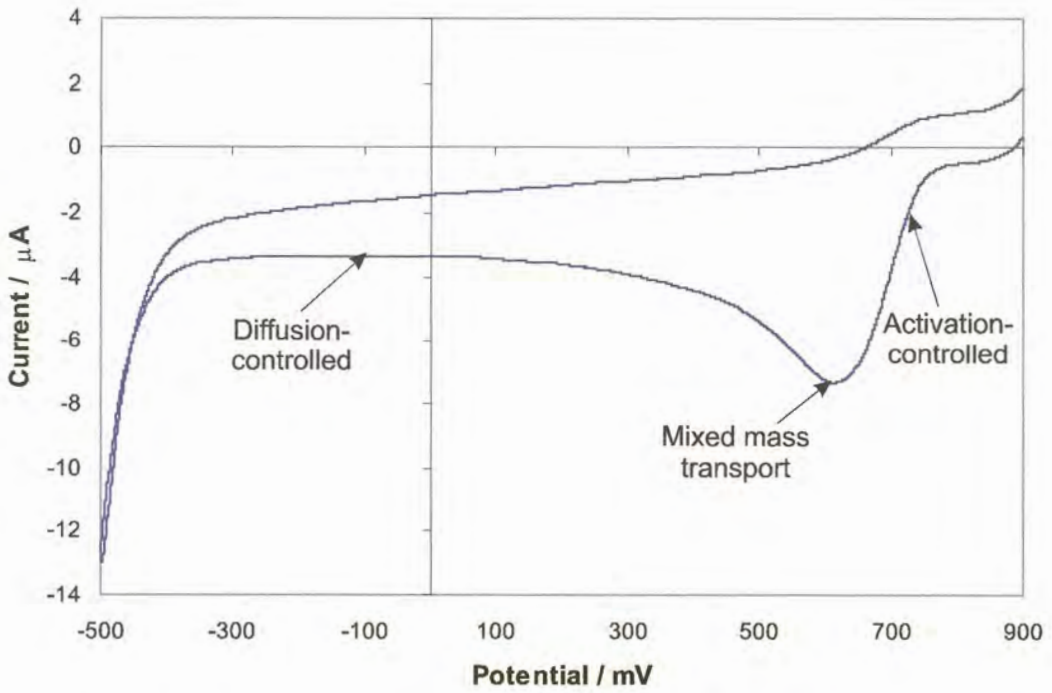

Figure 2.6: Cyclic voltammogram of the gold plating solution

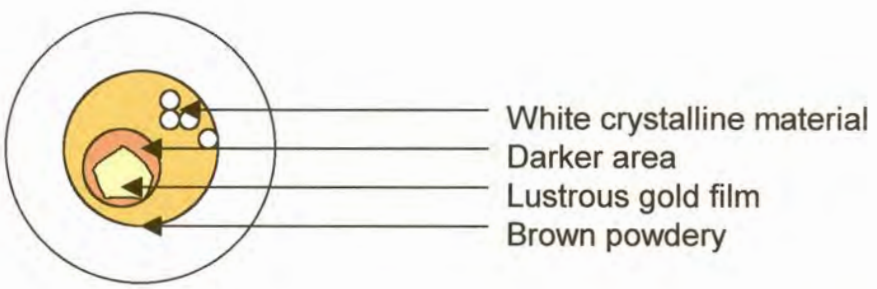

Figure 2.7: Gold film on the glassy carbon substrate at approximately 40 times magnification

After this rigorous polishing of the GCE, plating at –200 mV, as before, produced a lustrous dense gold film with a low resistance and doing a make-up run just after the plating of the film improved the reproducibility. Plating at 760 mV still produced a brownish deposit. It thus seems best to plate in the diffusion controlled region.

At a later stage during the project, it was found that the polishing procedure adopted did not sufficiently regenerate the GCE surface. An electrochemical treatment of the GCE was then investigated. It was found that applying a step function with a sample width of 250 ms between –700 mV and 700 mV for 1000 cycles in the gold plating solution produced the best results. The gold film was then plated as before.

2.1.2.3) Results

In order to produce a dense lustrous uniform gold film on a glassy carbon substrate, the developed procedure was summarised in point form below.

1) The GCE was polished with 1 μm alumina, rinsed with water and then ultrasonicated in water for about a minute. The electrode was then rinsed successively in water, 1 mol.l^{-1} nitric acid and water again.
2) If the deposited film was not uniform, a more rigorous polishing program was established. It included polishing successively with 9 μm, 3 μm and 1 μm diamond paste, with rinsing and ultrasonicating between the different size abrasives. Lastly the electrode was polished with 1 μm alumina as described above.
3) The plating solution for the gold film electrode was a 50 mg.l^{-1} gold solution in 5% (v/v) sulphuric acid. This was obtained by dissolving 99.99% gold in aqua regia to produce a 10 g.l^{-1} gold solution. It was then diluted and the appropriate amount of sulphuric acid was added.
4) Plating took place in a vial that was filled with 8 ml of gold plating solution. The solution was sparged with nitrogen for 5 minutes before plating commenced and a nitrogen blanket was maintained above the surface of the solution during plating. The GCE was lifted and reinserted in and out of the solution about three times after sparging to remove any bubbles lodged on the electrode surface.
5) The gold film was plated at –200 mV for 4 minutes in a stationary solution.
6) A gold make-up plating run was done straight after plating and when the electrode was starting to loose sensitivity. This was done similarly to the plating step, but a potential of 500 mV was applied for 5 s.
7) The plated electrode could be stored in a deoxygenated solution of 0.1 mol.l^{-1} sulphuric acid overnight. It was best to do a make-up run before starting analyses.

8) As the sensitivity of the gold film electrode does degrade with use, it may be useful to periodically include a check standard to assess the situation.
9) When the polishing procedure was not sufficient to regenerate the GCE surface, an electrochemical treatment was utilised. Applying a step function of sample width 250 ms between –700 mV and 700 mV `for 1000 cycles in the gold plating solution yielded the best results. The gold film was then plated as before.

2.2) REFERENCE ELECTRODES

The BAS RE-5 (MF-2063) Ag/AgCl reference electrodes were used in this work. An electrode is 7.5 cm long with an outer diameter of 6 mm. It has a Vycor tip and is filled with a 3 mol.l^{-1} NaCl solution saturated with AgCl. The viability of the reference electrodes were tested as suggested by the BAS Electrode Polishing and Care leaflet [17]. This was done due to the reported difficulties reference electrodes experience in solutions of high ionic strength [18]. The reference electrode in question, together with another reference electrode of the same type, was inserted into a beaker containing 3 mol.l^{-1} NaCl. They were then connected to a voltmeter and the potential difference was read. Ideally for electrodes of the same kind the potential difference should be zero, but there is some variation in practice. An acceptable reading is given as 0 $\pm$ 20 mV [17]. If there is a discrepancy, the electrodes could be compared to a third electrode to see which electrode is bad. Three of these electrodes were purchased simultaneously and were used in approximately two week cycles to maximise their lifetime.

2.3) AUXILIARY ELECTRODES

Platinum wire electrodes were used as the auxiliary electrodes in this work. The function of the auxiliary electrode is to allow current to flow through the electrolyte without influencing the measurement at the working electrode. Platinum is regularly used due to its low resistance and inert character.

2.4) REFERENCES

1) A.J. Bard, Electroanalytical Chemistry, Volume 16, Marcel Dekker Inc., 1989

2) P.T Kissinger and W.R. Heineman, Laboratory Techniques in Electroanalytical Chemistry, 2nd Edition, Marcel Dekker Inc., New York, 1996
3) Kh.Z. Brainina, Anal. Chim. Acta, 305 (1995) 146
4) D.C. Johnson, S.G. Weber, A.M. Bond, R.M. Wightman, R.E. Shoup and I.S. Krull, Anal. Chim. Acta, 180 (1986) 187
5) H. Eskilsson, C. Haraldsson and D. Jagner, Anal. Chim. Acta, 175 (1985) 79
6) I.G.R. Gutz, L Angnes and J.J. Pedrotti, Anal. Chem., 65 (1993) 500
7) W.M. Peterson, Reference unknown
8) J.J. Pedrotti, L. Angnes and I.G.R. Gutz, Anal. Chim. Acta, 298 (1994) 393
9) A.M. Bond, H.A. Hudson and P.A. van den Bosch, Anal. Chim. Acta, 127 (1981) 121
10) H.G. Jayaratna, C.S. Bruntlett and P.T. Kissinger, Anal. Chim. Acta, 332 (1996) 165
11) E.S. Pilkington, C. Weeks and A.M. Bond, Anal. Chem., 48 (1976) 1665
12) M. Florence, Analyst, 111 (1986) 489
13) A.M. Bond, Modern Polarographic Methods in Analytical Chemistry, Marcel Dekker Inc., 1980
14) A.Economou and P.R. Fielden, Trends in Anal. Chem., 16 (1997) 286
15) R.J. Rucki, Talanta, 27 (1980) 147
16) Model 303 Static Mercury Drop Electrode, Operating and Service Manual, 1978
17) BAS LCEC and EC Accessories, A-1302, Electrode Polishing and Care
18) A.M. Bond, H.A. Hudson, D.L. Luscombe, K.L. Timms and F.L. Walter, Anal. Chim Acta, 200 (1987) 213
19) Y.-C. Sun, J. Mierzwa and M.-H. Yang, Talanta, 44 (1997) 1379
20) P.Grundler and G.-U. Flechsig, Electrochim. Acta, 43 (1998) 3451
21) J.H. Aldstadt and A.F. Martin, Analyst, 121 (1996) 1387
22) G. Forsberg, J.W. O'Laughlin and R.G. Megargle, Anal. Chem., 47 (1975) 1586
23) M. Kopanica and L. Novotny, Anal. Chim. Acta, 368 (1998) 211
24) F.G. Bodewig, P. Valenta and H.W. Nurnberg, Fresenius J. Anal. Chem., 311 (1982) 187
25) P.H. Davis, G.R. Dulude, R.M. Griffin, W.R. Matson and E.W. Zink, Anal. Chem., 50 (1978) 137
26) T.W. Hamilton, J. Ellis and T.M. Florence, Anal. Chim. Acta, 119 (1980) 225
27) D. Jagner, M. Josefson and S. Westerlund, Anal. Chem., 53 (1981) 2144

28) J. Wang and B. Greene, J. Electroanal. Chem., 154 (1983) 261
29) A. Inoue, R.L. Earley, M.W. Lehmann and L.E. Welch, Talanta, 46 (1998) 1507
30) T.W. Hamilton, J. Ellis and T.M. Florence, Anal. Chim. Acta, 110 (1979) 87
31) W. Frenzel, Anal. Chim. Acta, 273 (1992) 123
32) F. Baumann and I. Shain, Anal. Chem., 29 (1957) 303
33) J. Wang and L.D. Hutchins, Anal. Chim. Acta, 167 (1985) 325
34) M. Korolczuk, Fresenius J. Anal. Chem., 357 (1997) 389
35) H. Gunasingham, K.P. Ang and C.C. Ngo, Anal. Chem., 57 (1985) 505
36) P.J. O'Connell, C.K. O'Sullivan and G.G. Guilbault, Anal. Chim. Acta, 373 (1998) 261
37) J. Wang and M. Ariel, J. Electroanal. Chem., 83 (1977) 217
38) M.M.P.M. Neto, M.M.G.S. Rocha and C.M.A. Brett, Talanta, 41 (1994) 1597
39) M.C. Sneed, J.L. Maynard and R.C. Brasted, Comprehensive Inorganic Chemistry II, D. von Nostrand Company, 1954

CHAPTER 3

FLOW CELLS

3.1) THEORY

There are a number of requirements that need to be met in order for an electrochemical detector to be reliable. The hydrodynamics through the flow cell needs to be reproducible. It need not be well-defined for analytical applications, but this does assist in the optimisation of parameters [1]. The dead volume, which is not necessarily the geometric volume, needs to be minimised [1]. The electrochemical cell should be easy to handle and maintain. The working electrode should be able to be removed in order to clean it. The electrode placement within the cell is also important. The electrodes need to be placed close together to reduce cell resistance and the counter electrode should be placed downstream from the working electrode to prevent reaction products from the counter electrode from interfering with the detection [1,2]. The reference electrode must be stable. The silver/silver chloride and calomel electrodes are the most frequently used reference electrodes in flow systems. The disadvantage with these electrodes is that a filling solution is used and it must be maintained at a constant concentration without cross-contamination from the bulk solution [1]. This problem can be overcome by using a salt bridge. In theory, an increase in the size of the working electrode surface should lead to an increased analytical signal. This does however also lead to an increase in noise and, in the case of a SMDE, the drop becomes physically unstable [3]. Hence a compromise pertaining to the electrode size needs to be reached.

3.2) FLOW CELL FOR A HMDE

An important aspect that should be borne in mind when designing a flow cell for a mercury drop electrode is that the flow through the cell must be laminar in order to minimise any effects from turbulence [4].

Many different flow cells were designed for the use of a HMDE. They considered factors such as laminar flow, mercury drop stability, removal of mercury waste from the cell and so on. These included simple designs, for example, that by Bond *et al.* in figure 3.1 [4], to more complex cells such as that by Alpizar *et al.* in figure 3.2 [3].

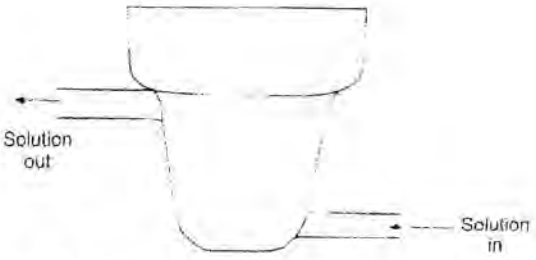

Figure 3.1: Flow cell with a volume of 30 ml to fit on a PARC Model 303 SMDE

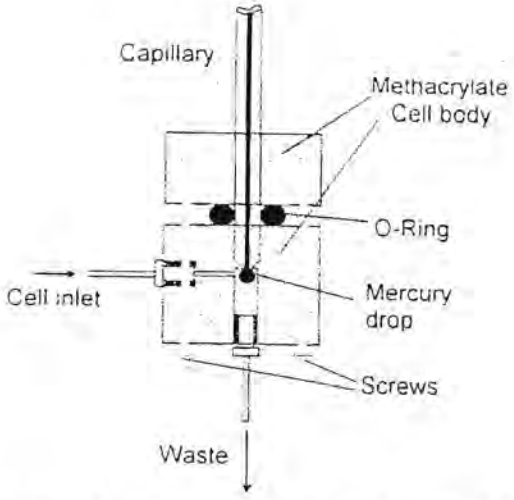

Figure 3.2: Flow cell with an Amel SMDE

Hanekamp *et al.* [2] looked at three types of mercury drop flow systems, namely:

1) parallel mercury and fluid flow

2) opposite mercury and fluid flow, and

3) mercury flow perpendicular to fluid flow.

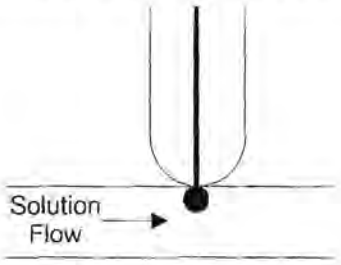

It was found that higher currents were obtained for opposite solution and mercury flow directions than for that in parallel directions, but the highest currents were obtained when the flow directions were perpendicular [2]. Hence the flow cell designed in this work had a perpendicular flow configuration. The mercury drop, which protruded into a horizontally flowing stream, was subjected to lateral forces that tended to displace it in the flow direction. This necessitated high flow rates to be avoided or else the mercury drop became unstable [4-6]. The reproducibility also decreases and the amount of noise increases at high flow rates, probably due to the mechanical instability of the mercury drop [4,5]. Saur *et al.* [7] found that the use of larger mercury drops increased the peak current to a greater extent in a flow cell with perpendicular flow than in a normal cup cell. This was due to the decrease of the

free channel cross-section which results in a locally increased flow speed. However, the use of larger mercury drops also leads to instability and irreproducibility. Thus a compromise between stability and sensitivity needs to be reached.

Stagnant areas of solution between the mercury drop and the capillary must be avoided. In figure 3.3 the stagnant areas are indicated in red [7]. It can be seen that perpendicular flow directions produce better results.

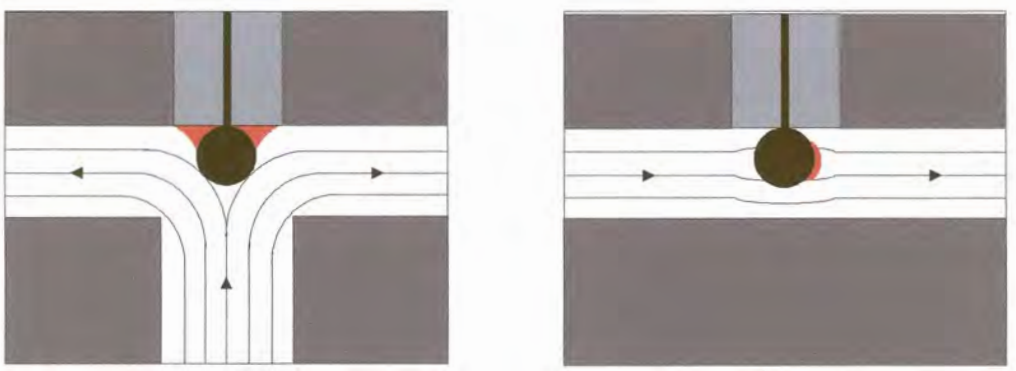

Figure 3.3: Flow geometry at a HMDE with a) opposite flow and b) perpendicular flow. The arrows and contours indicate the flow of the solution. The red areas indicate the stagnant areas.

3.2.1) Flow Cell for the SMDE for the Determination of Cobalt

The flow cell designed for this work is illustrated in figure 3.4. The flow cell is made from a polymethylmethacrylate (Perspex) cylinder as it is inert to the solutions used and in order to see what is happening inside during an analysis. There are spaces for the mercury capillary, a platinum wire for the auxiliary electrode and a BAS reference electrode. The reference electrode is placed after the working electrode to prevent any bleeding from interfering and it is also outside the electrical field between the working and counter electrodes [7].

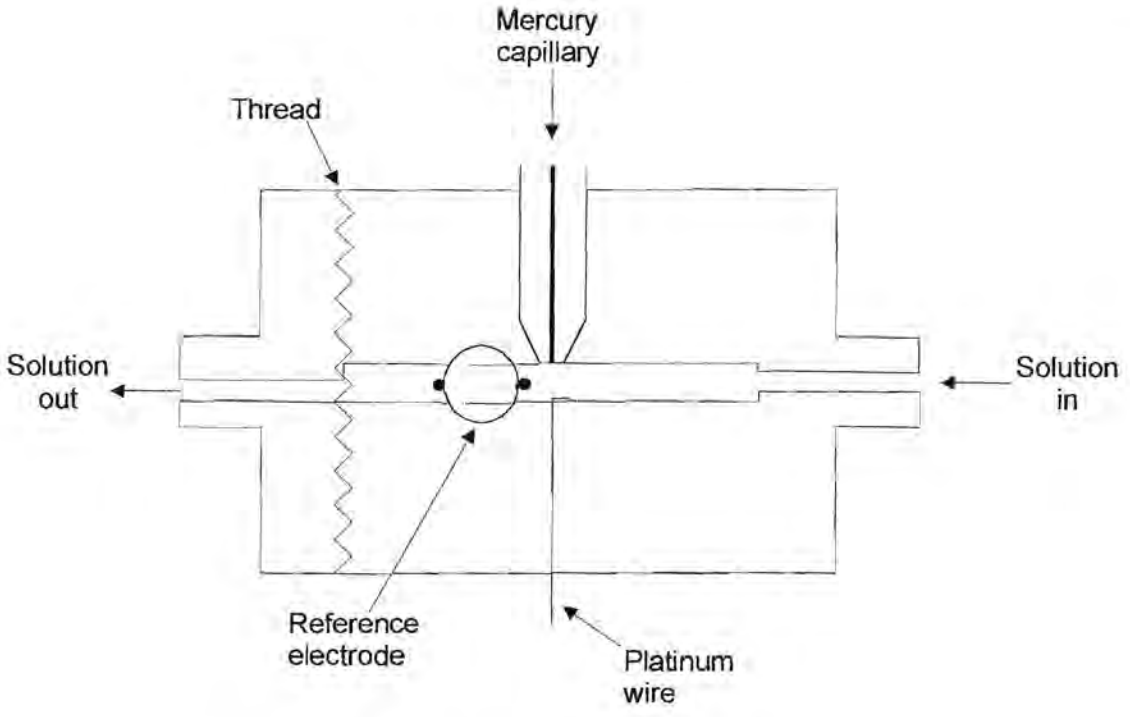

Figure 3.4: Flow cell for the SMDE

The platinum wire was sealed into place using an epoxy resin. This was later modified by soldering the platinum wire onto a brass screw and it was the screw to which a crocodile clip was then fastened (see figure 3.5). Both the platinum wire and the screw were sealed into place with epoxy resin.

The position of the platinum wire in the flow cell was also adjusted. Initially it was positioned just below the mercury drop in order to minimise the iR drop between these electrodes [8,9], but after a short time of use, the mercury formed an amalgam with the platinum and the mercury was not washed out of the flow cell. Instead it built up over the platinum until it merged with the mercury drop being dispensed from the capillary. It is generally specified that the counter electrode be place after the working electrode in the direction of flow in the cell so that the products generated at this electrode are not detected by the working electrode [8,10]. This may, however, have had a similar result. A few runs were done with a platinum wire situated before and after the working electrode in the zinc electrolyte that was to be analysed and no difference in the results were found.

The capillary was also initially sealed in place using silicone sealant, but later an o-ring was inserted to hold it firmly in place. The reference electrode was also held in place with two o-rings. In both cases, slight variations in size of the capillaries and reference electrodes necessitated that they be covered with some Teflon tape first to provide a good seal.

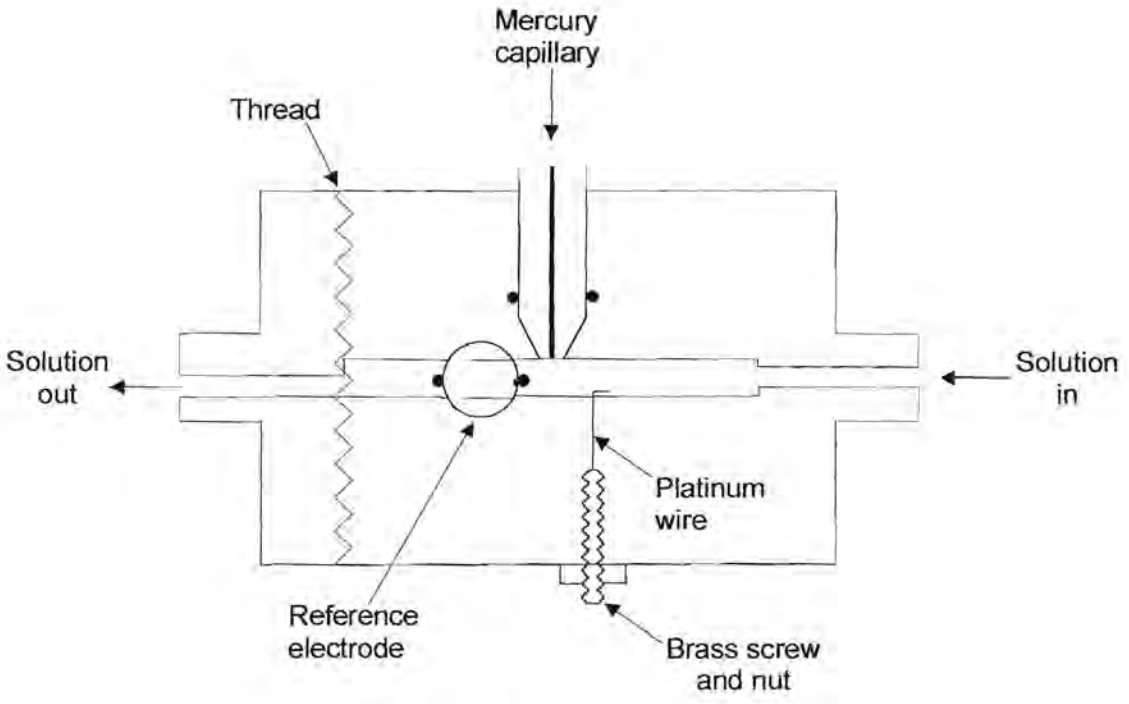

Figure 3.5: Modified flow cell for the SMDE

The dimensions of the flow cell are shown in figure 3.6. The diameter of the inlet is similar to that of the tubing through which the solution passed before it entered the flow cell. This was chosen so that the turbulence in flowing from the tubing to the flow cell would be minimal and also to assist in the joining of the tubing to the cell. The inner diameter is then increased so that there would be enough space for the solution to flow around the mercury drop hanging from the end of the capillary, but making sure that the amount of dead space is kept to a minimum. The cross-sectional area also needs to be kept small in order to increase the mean linear solution velocity [2,7]. Once again it was tried to minimise the turbulence by placing the entrance into the wider channel in the centre. Additionally, the most suitable flow rate would have to be determined to produce laminar flow for this particular cell. The exit from this channel is narrowed again to apply a back-pressure and is situated at

the bottom of the wide channel so that the used mercury drops could be easily washed out of the cell into waste. The outer diameter of the inlet is 5 mm in order to allow the tubing that was used in the deoxygenation system (see chapter 4) to fit tightly over it.

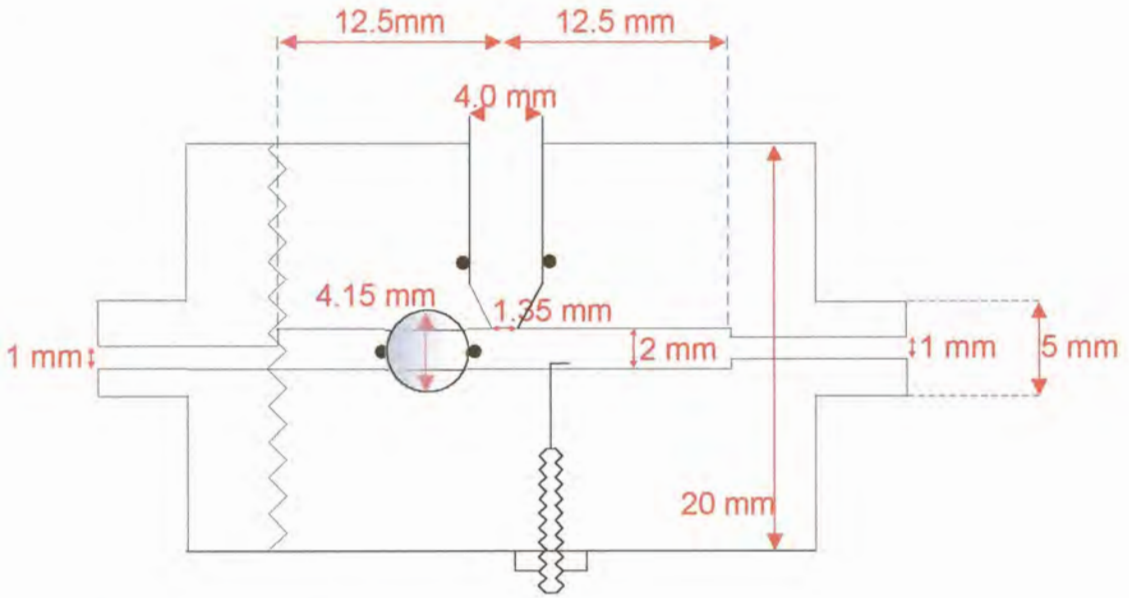

Figure 3.6: Flow cell dimensions

The end of the flow cell could be screwed off at the point indicated by the thread in figure 3.5. This was to allow the manufacturer to make a wide channel between the narrower inlet and outlet. This also assisted in inserting a wire to bend the platinum wire counter electrode flat against the side of the channel, so as not to obscure the path of the solution. When a significant back-pressure was applied, the cell started leaking at the thread, so a gasket made from a thick plastic sheet was inserted.

Another problem was that the drop knocker could not shake the capillary sufficiently to dislodge the mercury drop when it was in position in the flow cell. It was found that allowing an air bubble to pass through the cell dislodged the drop and carried it out into waste. Introducing air into the system would diminish previous deoxygenation as the oxygen would diffuse into the solution, so nitrogen was used instead.

This cell was used as part of the flow system described in chapter 5 for the determination of cobalt in a zinc electrolyte. The characteristics of the flow cell were also investigated in that chapter.

3.3) WALL-JET CELLS

A wall-jet is described as the flow of a jet of fluid that strikes a plane perpendicularly and flows radially over its surface [1,11-15]. It was noted that the velocity of the fluid in the direction normal to the electrode is towards the electrode at large distances from the electrode, but the flow is away from the electrode close to the electrode. The flow is zero along the surface given by:

$$\eta = 0.51\,k\left(\frac{V}{\nu}\right)^{3/4} a^{-1/2} r^{-5/4} z = 3.96$$

where V is the volume flow rate through the inlet, ν is the kinematic viscosity, a is the nozzle diameter, r is the radial distance, z is the distance normal to the electrode and k is equal to 0.86 [1,11,16]. This is illustrated in figures 3.7 and 3.8.

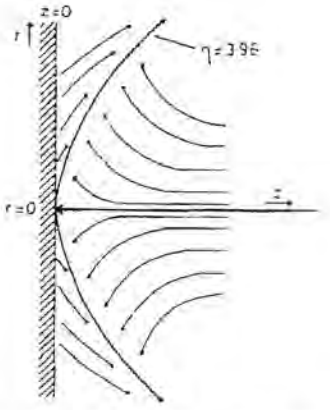

Figure 3.7: Velocity flow profiles at the wall-jet electrode (WJE) where r is the electrode radius, z is the direction normal to the electrode and η is the stagnant region [1]

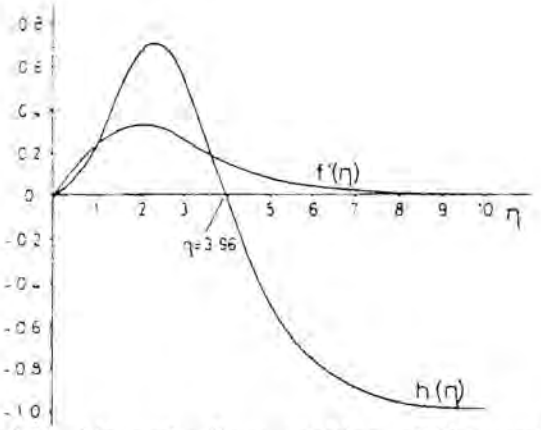

Figure 3.8: Velocity flow profiles at the wall-jet electrode (WJE) where f'(η) is the radial velocity profile and h(η) is the velocity profile normal to the electrode surface. η=3.96 is the stagnant region [1]

Laevers *et al.* [15] subdivided the flow pattern into 4 hydrodynamic regions, namely, the potential core, the free-jet region, the stagnation zone and the wall-jet region. These are depicted in figure 3.9. As solution flows from the submerged nozzle, the solution in the jet exchanges momentum with the surrounding fluid to create a free-jet. This forms a conical potential core which varies from 4 to 8 nozzle diameters in length, depending on the shape of the nozzle. Due to intensive momentum exchange, the jet broadens as it gets close to the electrode, up to a limiting distance of 1.2 to 2.2 nozzle diameters from the electrode surface, which is then the start of the stagnation zone. In the stagnation zone the flow is deflected by the electrode surface, its axial velocity is decelerated and transformed to an acceleration parallel to the surface. Due to the exchange of momentum with the quiescent surrounding fluid, the accelerating flow transforms into a decelerating wall-jet. The velocity parallel to the electrode surface reaches a maximum 0.6 to 1.4 nozzle diameters from the stagnation point, where the stagnation zone transforms into the wall-jet region. In the wall-jet region, the flow is influenced by both the quiescent surrounding fluid and the electrode surface [15].

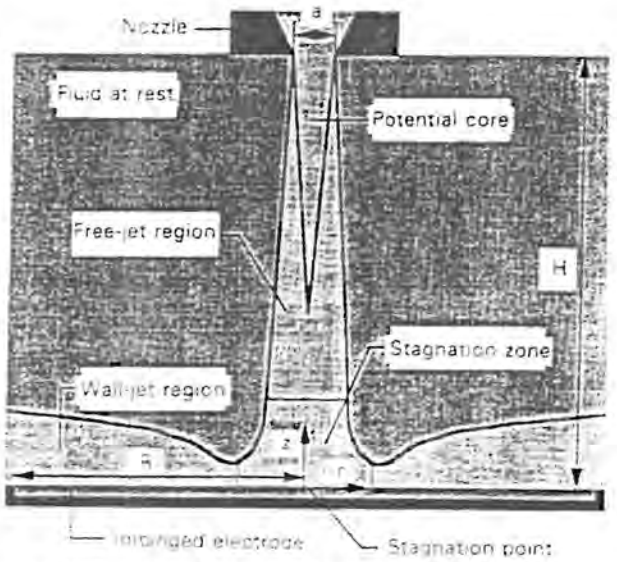

Figure 3.9: The flow pattern in a WJE [15]

This flow pattern clearly shows that the WJE is not uniformly accessible as the rate of mass transport is higher towards the centre of the electrode than at the edge [1,14,15]. Only fresh solution from the jet reaches the electrode surface, not the dead solution in the cell chamber. Therefore it is not necessary to flush out the cell compartment between analyses [11,16,17].

The mass transport of electroactive species (*i*) to the impinged surface of the WJE can be described by the convective diffusion equation:

$$\frac{\partial C_i}{\partial t} = D_i \frac{\partial^2 C_i}{\partial z^2} - v_r \frac{\partial C_i}{\partial r} - v_z \frac{\partial C_i}{\partial z}$$

where r and z are the distances along and normal to the electrode in cylindrical pole coordinates with the origin at the intersection of the jet axis and the electrode surface, v_r and v_z are the corresponding velocity components and D_i is the diffusion coefficient of *i* [18]. Two assumptions were made to reach this equation, namely that homogeneous reactions producing or consuming *i* do not occur and radial diffusion is omitted. Radial diffusion effects only become important where the solution is most stagnant which occurs at the outer radius of the electrode. However, in this region the radial concentration gradients are small, thus the effect of radial diffusion on concentration changes can be neglected [18].

The limiting current can be calculated by:

$$i_{lim} = 1.38nFCD^{2/3}\nu^{-5/12}V^{3/4}a^{-1/2}R^{3/4}$$

where n is the number of electrons, F is Faraday's constant, C is concentration, D is the diffusion coefficient, ν is the kinematic viscosity, V is the flow rate, a is the nozzle diameter and R is the electrode radius [15,16,19]. Although the equation does not include a term for the separation between the inlet nozzle and the electrode surface, it is assumed that the jet does not break up before it impinges in the electrode [1,15,19].

When a fluid flows over the electrode surface, a very thin layer is formed at the surface where the velocity gradient normal to the surface is very large. This layer is called the boundary layer [1,20]. The boundary layer thickness for the WJE is calculated as follows:

$$\delta_{bl} = 5.8\pi^{3/4}a^{1/2}\nu^{3/4}x^{5/4}V^{-3/4}$$

where a is the inlet diameter, ν is the kinematic viscosity, x is the electrode radius and V is the flow rate [19,21]. From this it can be deduced that the boundary layer thickness increases rapidly from the centre of the electrode to the outer edge and that it decreases rapidly as the flow rate increases.

The diffusion layer thickness is calculated by:

$$\delta_{dl} = 5.8k_2\pi^{3/4}D^{1/3}a^{1/2}\nu^{5/12}x^{5/4}V^{-3/4}$$

where $k_2 = 0.17$. It is estimated that the diffusion layer is 2% of the hydrodynamic boundary layer thickness [16,19].

When considering the design of a wall-jet cell (WJC), there are a number of factors to take into consideration. Some of these are listed below.

1) In order to maintain true wall-jet behaviour, there should be no interference with the development of the boundary layer in a WJC, therefore the nozzle body, the back wall, the counter electrode and the reference electrode should not be located close to the working electrode [1,16]. The bulk volume of the cell should also be large [16]
2) The jet formed should be stable, preferably with laminar flow characteristics [16].

3) The proportionality between the limiting current and the flow rate is obeyed only when the inlet-electrode separation is greater than a certain value which is governed by several factors such as electrode diameter, solution flow rate, solution viscosity and the geometry of the nozzle body [19].
4) Laevers *et al.* [15] found that for true wall-jet behaviour the following relationship between the nozzle diameter (a) and the nozzle-electrode separation (H) should hold:

$$12 \leq H/a \leq 15$$

If the ratio of H:a is too small, the jet does not fully develop before it strikes the electrode surface and if the ratio is too large, the free-jet spreads out before it impinges on the electrode surface.
5) The diameter of the free-jet should be negligible, therefore the electrode diameter should be at least 10 times larger than that of the inlet diameter [1,16].

3.3.1) Wall-Jet Cell used for the Determination of Arsenic in Gold

The cell designed for this work is illustrated in figure 3.10 and the measurements are shown in figure 3.11. As for the previous cell, this flow cell was made from a polymethylmethacrylate (Perspex) cylinder as it is inert to the solutions used and in order to see what is happening inside during an analysis. There are cavities for a BAS glassy carbon electrode, a platinum wire for the auxiliary electrode and a BAS reference electrode. The platinum wire was soldered to a brass screw and they were sealed into place with epoxy resin. The top and the bottom parts of the flow cell were held together by three bolts (not depicted in the diagram) with an o-ring between to make a good seal. An o-ring held the working electrode in place, so it was easy to adjust the inlet-electrode separation and it could be readily removed to clean. The reference electrode was separated from the cell compartment by a narrow passage which extended the life of this electrode. An outlet was situated in the reference electrode compartment so the solution around the electrode could be renewed. Another outlet was situated at the top of the conical section of the cell for the facile removal of bubbles. The inlet was made from PEEK (polyetheretherketone) and had an inner diameter of 0.3 mm.

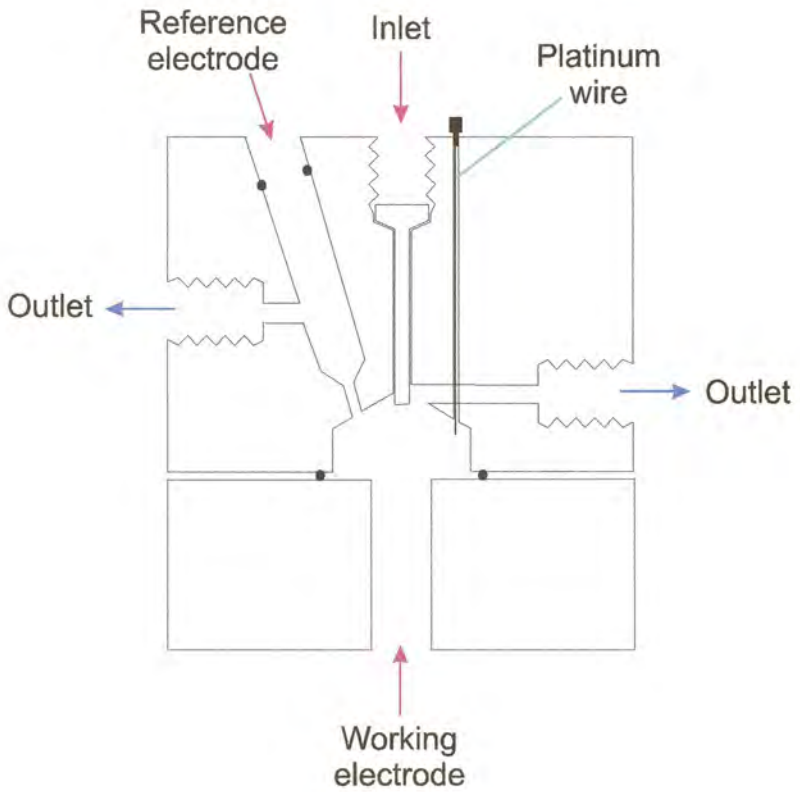

Figure 3.10: Wall-jet cell

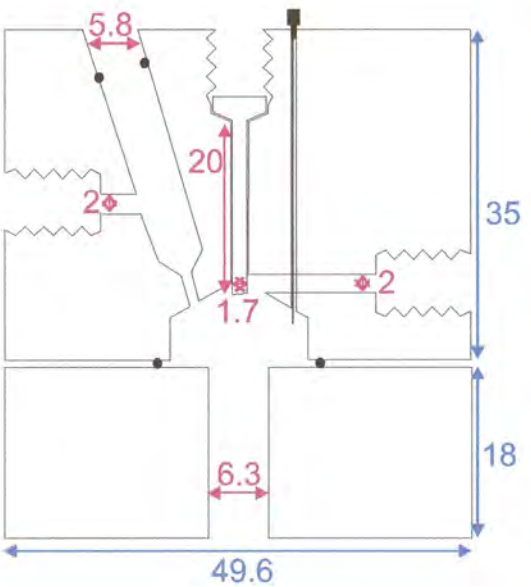

Figure 3.11: Dimensions of the wall-jet cell (values quoted in mm)

The volume of the cell was approximated by calculating the geometric volume from the dimensions. This is shown in figure 6.12.

Figure 3.12: The geometric sections of the cell cavity used to calculate its volume

Total volume = volume of cylinder + volume of pyramid

$= \pi r^2 h + 1/3\pi r^2 h$

$= 795.2\ mm^3 + 217.9\ mm^3$

$= 1013.1\ mm^3$

Therefore the estimated volume is 1 ml. This is a relatively large volume as the volume for thin layer cells is generally of the order of a few µl. There should be no interference with the development of the boundary layer with these cell dimensions. In the case of a WJC, the dead volume is not the same as the geometric volume. It is preferable to have a large geometric volume for a WJC.

3.4) REFERENCES

1) A.J. Bard, Electroanalytical Chemistry, Volume 16, Marcel Dekker Inc., 1989
2) H.B. Hanekamp and H.J. van Nieuwkerk, Anal. Chim. Acta, 121 (1980) 13
3) J. Alpizar, A. Cladera, V. Cerda, E. Lastres, L. Garcia and M. Catasus, Anal. Chim. Acta, 340 (1997) 149
4) A.M. Bond, H.A. Hudson and P.A. van den Bosch, Anal. Chim. Acta, 127 (1981) 121
5) L.A. Mahoney, J. O'Dea and J.G. Osteryoung, Anal. Chim. Acta, 281 (1993) 25
6) U. Baltensperger and R. Eggli, Anal. Chim. Acta, 123 (1981) 107
7) D. Sauer and E. Spahn, Fresenius J. Anal. Chem., 351 (1995) 154
8) W. Lund and L.-N. Opheim, Anal. Chim. Acta, 79 (1979) 35
9) D.C. Johnson, S.G. Weber, A.M. Bond, R.M. Wightman, R.E. Shoup and I.S. Krull, Anal. Chim. Acta, 180 (1986) 187

10) J.A. Wise, W.R. Heineman and P.T. Kissinger, Anal. Chim. Acta, 172 (1985) 1
11) W.J. Albery and C.M.A. Brett, J. Electroanal. Chem., 148 (1983) 211
12) W.J. Albery and C.M.A. Brett, J. Electroanal. Chem., 148 (1983) 201
13) J. Wang and B.A. Freiha, Anal. Chem., 57 (1985) 1776
14) R.G. Compton, A.C. Fisher, M.H. Latham, R.G. Wellington, C.M.A. Brett and A.M.C.F. Oliveira Brett, J. Appl. Electrochem., 23 (1993) 98
15) P. Laevers, A. Hubin, H Terryn and J. Vereecken, J. Appl. Electrochem., 25 (1995) 1017
16) H. Gunasingham, K.P. Ang, C.C. Ngo, P.C. Thiak and B. Fleet, J. Electroanal. Chem., 186 (1985) 51
17) H. Gunasingham, K.P. Ang, C.C. Ngo and P.C. Thiak, J. Electroanal. Chem., 198 (1986) 27
18) P. Laevers, A. Hubin, H Terryn and J. Vereecken, , J. Appl. Electrochem., 25 (1995) 1023
19) H. Gunasingham and B. Fleet, Anal. Chem., 55 (1983) 1409
20) R.J. Rucki, Talanta, 27 (1980) 147
21) H. Gunasingham, Anal. Chim. Acta, 159 (1984) 139